Journal of Sensor Science and Technology
Vol. 28, No. 3 (2019) pp. 152-156
http://dx.doi.org/10.5369/JSST.2019.28.3.152
pISSN 1225-5475/eISSN 2093-7563

GaN-based Ultraviolet Passive Pixel Sensor for UV Imager

Chang-Ju Lee, Sung-Ho Hahm, and Hongsik Park+

Abstract

An ultraviolet (UV) image sensor is an extremely important optoelectronic device used in scientific and medical applications because it can detect images that cannot be obtained using visible or infrared image sensors. Because photodetectors and transistors are based on different materials, conventional UV imaging devices, which have a hybrid-type structure, require additional complex processes such as a backside etching of a GaN epi-wafer and a wafer-to-wafer bonding for the fabrication of the image sensors. In this study, we developed a monolithic GaN UV passive pixel sensor (PPS) by integrating a GaN-based Schottky-barrier type transistor and a GaN UV photodetector on a wafer. Both individual devices show good electrical and photoresponse characteristics, and the fabricated UV PPS was successfully operated under UV irradiation conditions with a high on/off extinction ratio of as high as 10^3. This integration technique of a single pixel sensor will be a breakthrough for the development of GaN-based optoelectronic integrated circuits.

Keywords: GaN, UV sensor, SB-MOSFET, UV PPS, UV image sensor

1. INTRODUCTION

Over the last two decades, GaN-based electrical devices have been actively studied for high-power and high-frequency device applications. In recent years, many research groups have intensively studied enhancement-mode GaN-channel MOSFETs for implementation in high-efficiency power electronic systems [1-3]. In particular, owing to their normally off mode operation and low-power consumption, Si-doped source/drain-type and Schottky-barrier (SB) GaN MOSFETs have been studied with regard to their use in optoelectronic integrated circuits [4-9]. GaN has a wide bandgap of 3.4 eV, which corresponds to the ultraviolet (UV) wavelength region, and thus the material can be widely used for UV light-emitting devices and UV sensor applications. The commercial applications of UV sensors are continuing to grow, particularly in the areas of healthcare, ozone-layer monitoring, and fire alarms. During the last decade, various types of GaN-based UV sensors and other material-based UV sensors have been proposed [10-15]. Among such structures, a metal-semiconductor-metal (MSM) UV sensor has been extensively studied owing to its simpler fabrication process, lower dark current density, and higher process compatibility with GaN-based transistors than other sensor structures.

In conventional UV imaging devices, a hybrid-type structure is typically used [16]. To fabricate this hybrid structure, additional complex processes are required during device fabrication, such as the backside etching of the GaN epi-wafer substrate and wafer-to-wafer bonding, because the photodetectors and transistors are based on GaN and silicon, respectively.

In this study, to investigate the possibility of a GaN-based UV imager integrated on a chip, we demonstrate the operation of a GaN-based UV passive pixel sensor (PPS) through the integration of a GaN MSM UV sensor and a GaN SB-MOSFET on an unintentionally doped GaN layer grown on a sapphire substrate. The GaN MSM UV sensor is used for the UV light detection part, and the GaN SB-MOSFET is used for the electrical switching part, of a single pixel sensor. We demonstrate the electrical and photoresponse characteristics of individual devices and the output characteristics of the fabricated UV PPS under dark and UV irradiation conditions.

2. EXPERIMENTAL

An unintentionally doped GaN layer was epitaxially grown on a (0001) sapphire substrate using metal–organic chemical vapor deposition. First, a 0.5-μm low-temperature GaN buffer layer was

School of Electronics Engineering, Kyungpook National Unversity
80 Daehakro, Buk-gu, Daegu, 41566, Korea
+Corresponding author: hpark@ee.knu.ac.kr
(Received: May 25, 2019, Revised: May 29, 2019, Accepted: May 30, 2019)

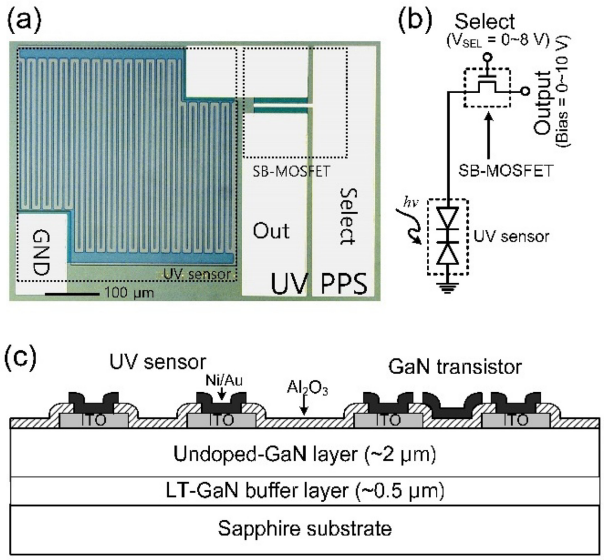

Fig. 1. (a) Micro-photograph image with the pad electrode names (scale bar, 100 μm), (b) circuit schematic, and (c) cross-sectional view with the epitaxial layer structure of the proposed GaN UV PPS.

grown, followed by a 2-μm-thick GaN layer grown at 1,070 °C. The total growth pressure of the proposed structure was fixed at 100 Torr. Fig. 1(a) shows a micro-photograph of the proposed GaN UV PPS. In an MSM-type UV sensor, a back-to-back connection of two Schottky diodes is used for a UV photodetector, and an SB-MOSFET is used for the current transfer controller. A circuit schematic and a cross-sectional view along with the epitaxial layer structure of the proposed GaN UV PPS are shown in Figs. 1(b) and 1(c), respectively.

For the Schottky metal electrodes of the MSM UV sensor and SB-MOSFET, a 100-nm-thick ITO was deposited using a radio-frequency magnetron sputtering system at 300 °C. During the deposition, the deposition condition was maintained at 10 mTorr under Ar/O_2 ambient conditions ($Ar:O_2$ = 1000:1). To form a gate insulator, a 17-nm-thick Al_2O_3 layer was deposited using an atomic layer deposition (ALD) system at 350 °C. After the Al_2O_3 layer was patterned and etched to form the contact holes, Ni (20 nm) and Au (50 nm) layers were deposited for the contact pad electrodes of the SB-MOSFET and the MSM UV sensor using an e-beam evaporator. The area of the UV sensor was 400 × 400 μm^2 with a finger length of 360 μm, a finger width of 5 μm, and a space of 10 μm, whereas that of the SB-MOSFET was 100 × 110 μm^2, with a gate length of 10 μm and a width of 100 μm. The electrical properties of the MSM UV sensor and the SB-MOSFET were characterized using an Agilent 4156C semiconductor parameter analyzer. For the measurement of the photoresponsive I–V characteristics, a monochromatic 365-nm UV light source was applied. The spectral photoresponsivity characteristic was measured using a 150-W xenon arc lamp with a monochromator system (Oriel 74000) and a Newport low-power detector. The optical power density of the monochromatic 365-nm UV light source was 447 mW/cm^2.

3. RESULTS AND DISCUSSIONS

A GaN SB-MOSFET has a unique operation characteristic differing from that of a conventional MOSFET. The Schottky barrier height of the source/drain contacts can be controlled using the gate-overlapped regions, as shown in Fig. 2, which makes the on/off operation of the GaN SB-MOSFET possible. Because the device structures of the GaN MSM UV sensor and GaN SB-MOSFET are the same, with the exception of the gate electrode, these two devices can be monolithically integrated on a GaN epitaxial wafer.

Fig. 3(a) shows the dark and photoresponsive I–V characteristics of the fabricated GaN MSM UV sensor, where the dark current was 4.2 × 10^{-5} A and the photoresponsive current was

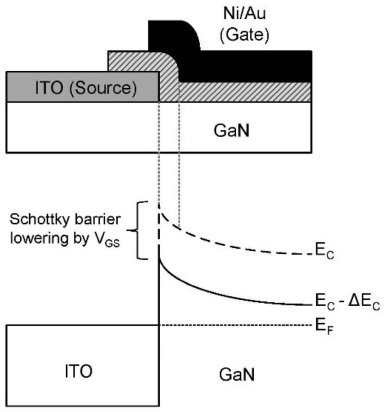

Fig. 2. Energy band structure of metal (ITO)/GaN contact interface with a Schottky barrier lowering effect using the gate bias at the gate overlapped region of the source contact.

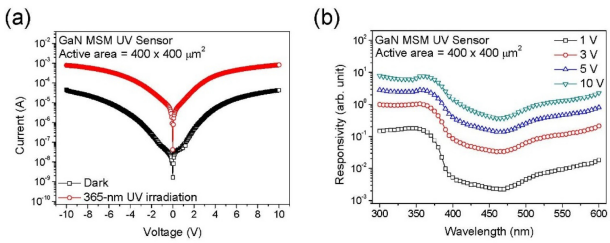

Fig. 3. (a) Dark and photoresponsive I–V characteristics and (b) spectral photoresponsivity characteristics of the fabricated GaN MSM UV sensor. The optical power density of a 365-nm UV light was 447 mW/cm^2.

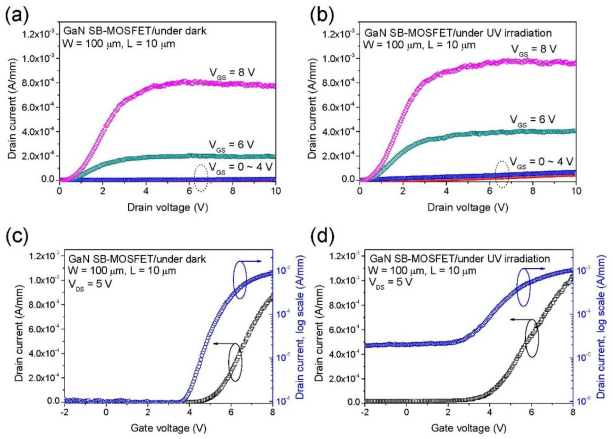

Fig. 4. (a) Output I_{DS}–V_{DS} characteristics under dark, (b) output I_{DS}–V_{DS} characteristic under 365-nm UV irradiation, (c) linear and log-scale transfer I_{DS}–V_{GS} characteristics under dark, and (d) linear and log-scale transfer I_{DS}–V_{GS} characteristics under 365-nm UV irradiation of the fabricated GaN SB-MOSFET. The optical power density of a 365-nm UV light was 447 mW/cm^2.

8.1×10^{-4} A at 10 V. The photo-to-dark contrast ratio was only 20 at 10 V, which was attributed to the high level of leakage current under a dark-state caused by a low Schottky barrier height at the ITO/GaN contact interface. Fig. 3(b) shows the spectral photoresponsivity of the fabricated GaN MSM UV sensor under different bias conditions of 1 to 10 V. The UV/visible rejection ratio, the ratio of the responsivity values for 365-nm and 450-nm wavelength, was lower than 10^2 under all bias conditions; this low rejection ratio is similar to the photo-to-dark contrast ratio of the fabricated UV sensor shown in Fig. 3(a), which can be explained based on the same reason mentioned above.

Fig. 4(a) shows the output I_{DS}–V_{DS} characteristic of the fabricated GaN SB-MOSFET. The maximum drain current was 0.8 mA/mm at V_{DS} = 10 V and V_{GS} = 8 V. In this experiment, the transistor region was not entirely covered by Ni/Au pad electrodes. To investigate the UV irradiation effect on the output characteristics of the fabricated GaN SB-MOSFET, we measured the output I_{DS}–V_{DS} characteristics under 365-nm UV irradiation, as shown in Fig. 4(b). In the saturation region, the on-state drain current was increased from 0.8 to 1.0 mA/mm and the off-state current was also slightly increased by the UV irradiation.

This small variation could affect the PPS operation; therefore, it should be solved for better device performance of the proposed GaN UV PPS through the optimization of the device fabrication process.

Fig. 4(c) shows the linear and log-scale transfer I_{DS}–V_{GS} characteristics of the fabricated GaN SB-MOSFET, where a

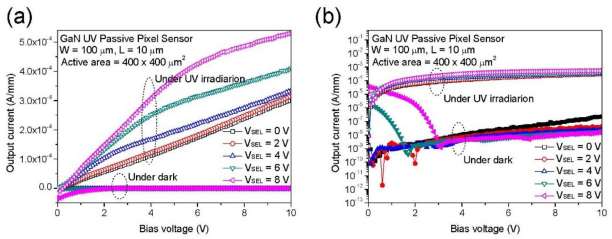

Fig. 5. (a) Linear-scale and (b) log-scale output I–V characteristics of the fabricated GaN UV PPS with/without 365-nm UV irradiation. The GaN UV PPS was fabricated by integration of a GaN MSM UV sensor and a GaN SB-MOSFET.

threshold voltage was 5.2 V, the current on/off ratio was 10^3, and the maximum transconductance was 0.5 mS/mm at V_{DS} = 5 V. To check the UV irradiation effect on the transfer characteristics of the SB-MOSFET for the same reason mentioned above, we measured the transfer I_{DS}–V_{GS} characteristics under 365-nm UV irradiation, as shown in Fig. 4(d).

Under the same bias conditions as with UV irradiation, the threshold voltage was shifted to 3.9 V, the current on/off ratio was dramatically decreased to 50 with an increase in the off-state drain current below the subthreshold region, and the maximum transconductance was slightly changed to 0.48 mS/mm. The main reason for these changes might be attributed to the uncovered region of the transistor area. Using these two devices, we implemented a GaN UV PPS on an epitaxially grown GaN wafer. An MSM UV sensor was used for the UV photodetector, and an SB-MOSFET was used for the current transfer controller. Figs. 5(a) and 5(b) show the linear and log-scale output I–V characteristics of the fabricated GaN UV PPS with/without 365-nm UV irradiation, respectively. A gate electrode of the SB-MOSFET was used for a select (SEL) electrode and a drain electrode was used for an output (OUT) electrode. In addition, V_{SEL} (0–8 V, step size of 2 V) was applied to the SEL electrode and a 0–10 V bias sweep was applied to the OUT electrode. Under a dark-state, the output current was 10^{-10}–10^{-7} A at V_{SEL} = 0–4 V and V_{OUT} = 0–10 V.

However, when the V_{SEL} was higher than 6 V, the output current changed from a highly negative to a low positive value according to the increase in the bias voltage, which is related to the gate leakage current at the gate-overlapped region of the source/drain electrodes. In contrast, under 365-nm UV irradiation, the output current was typically three orders of magnitude higher than that of the dark state when the bias voltage was increased. The on/off output current ratio was 10^3 for 365-nm UV irradiation under a 3–10 V bias; therefore, a UV on/off state is clearly distinguishable within this range of bias conditions. As shown in Fig. 5(a), the

gate controllability is the main issue of the fabricated GaN UV PPS under UV irradiation, which might be attributed to the photogenerated carriers at the uncovered region of the SB-MOSFET. This problem can be solved through the optimization of a layout design and the device fabrication process.

4. CONCLUSIONS

We demonstrated a GaN UV PPS through the integration of an MSM-type GaN UV sensor as an UV-photodetector and a GaN SB-MOSFET as a signal transfer controller. The fabricated GaN UV PPS showed a good UV response with an on/off ratio of higher than 10^3 at a 10 V bias and a low gate controllability under UV irradiation owing to the photogenerated carriers in the uncovered regions of the SB-MOSFET. If we optimize the metal/GaN Schottky contact characteristics and the fabrication process design for individual devices of both the GaN MSM UV sensor and the GaN SB-MOSFET, we can obtain a more improved device performance for the proposed GaN UV PPS, such as a low dark current, a high on/off ratio, and a high gate controllability under UV irradiation. Furthermore, we will be able to apply an active-type UV pixel sensor through the integration of the GaN MSM UV sensor and GaN SB-MOSFETs.

ACKNOWLEDGMENT

This work was supported in part by a National Research Foundation of Korea (NRF) grant funded by the Korean government (MSIT) (2017R1A4A1015565) and the Bio & Medical Technology Development Program of the NRF funded by the Ministry of Science & ICT (2017M3A9G8083382).

REFERENCES

[1] S. Sugiura, Y. Hayashi, S. Kishimoto, T. Mizutani, M. Kuroda, T. Ueda, and T. Tanaka, "Fabrication of normally-off mode GaN and AlGaN/GaN MOSFETs with HfO_2 gate insulator", *Solid-State Electron.*, Vol. 54, No. 1, pp. 79-83, 2010.

[2] K. S. Im, J. B. Ha, K. W. Kim, J. S. Lee, D. S. Kim, S. H. Hahm, and J. H. Lee, "Normally Off GaN MOSFET Based on AlGaN/GaN Heterostructure with Extremely High 2DEG Density Grown on Silicon Substrate", *IEEE Electron Device Lett.*, Vol. 31, No. 3, pp. 192-194, 2010.

[3] D. S. Kim, K. S. Im, K. W. Kim, H. S. Kang, D. K. Kim, S. J. Chang, Y. Bae, S. H. Hahm, S. Cristoloveanu, and J. H. Lee, "Normally-off GaN MOSFETs on insulating substrate", *Solid-State Electron.*, Vol. 90, pp. 79-85, 2013.

[4] W. Huang, T. Khan, and T. P. Chow, "Enhancement-Mode n-Channel GaN MOSFETs on p and n-GaN/Sapphire Substrates", *IEEE Electron Device Lett.*, Vol. 27, No. 10, pp. 796-798, 2006.

[5] H. Kambayashi, Y. Niiyama, S. Ootomo, T. Nomura, M. Iwami, Y. Satoh, S. Kato, and S. Yoshida, "Normally Off n-Channel GaN MOSFETs on Si Substrates Using an SAG Technique and Ion Implantation", *IEEE Electron Device Lett.*, Vol. 28, No. 12, pp. 1077-1079, 2007.

[6] Y. C. Chang, W. H. Chang, H. C. Chiu, L. T. Tung, C. H. Lee, K. H. Shiu, M. Hong, J. Kwo, J. M. Hong, and C. C. Tsai, "Inversion-channel GaN metal-oxide-semiconductor field-effect transistor with atomic-layer-deposited Al_2O_3 as gate dielectric", *Appl. Phys. Lett.*, Vol. 93, No. 5, pp. 053504(1)-053504(3), 2008

[7] D. K. Kim, D. S. Kim, S. J. Chang, C. J. Lee, Y. Bae, S. Cristoloveanu, J. H. Lee, and S. H. Hahm, "Performance of GaN Metal–Oxide–Semiconductor Field-Effect Transistor with Regrown n+-Source/Drain on a Selectively Etched GaN", *Jpn. J. Appl. Phys.*, Vol. 52, No. 6R, pp. 061001(1) 061001(5), 2013.

[8] H. B. Lee, H. I. Cho, H. S. An, Y. H. Bae, M. B. Lee, J. H. Lee, and S. H. Hahm, "A Normally Off GaN n-MOSFET With Schottky-Barrier Source and Drain on a Si-Auto-Doped p-GaN/Si", *IEEE Electron Device Lett.*, Vol. 27, No. 2, pp. 81-83, 2006.

[9] D. S. Kim, T. H. Kim, C. H. Won, H. S. Kang, K. W. Kim, K. S. Im, Y. S. Lee, S. H. Hahm, J. H. Lee, J. H. Lee, J. B. Ha, Y. Bae, and S. Cristoloveanu, "Performance enhancement of GaN SB-MOSFET on Si substrate using two-step growth method", *Microelectron. Eng.*, Vol. 88, No. 7, pp. 1221-1224, 2011.

[10] T. Tut, T. Yelboga, E. Ulker, and E. Ozbay, "Solar-blind AlGaN-based p-i-n photodetectors with high breakdown voltage and detectivity", *Appl. Phys. Lett.*, Vol. 92, No. 10, pp. 103502(1)-103502(3), 2008.

[11] X. D. Wang, W. D. Hu, X. S. Chen, J. T. Xu, X. Y. Li, and W. Lu, "Photoresponse study of visible blind GaN/AlGaN p-i-n ultraviolet photodetector", *Opt. Quantum Electron.*, Vol. 42, No. 11-13, pp. 755-764, 2011.

[12] K. H. Lee, P. C. Chang, S. J. Chang, and S. L. Wu, "GaN-based Schottky barrier ultraviolet photodetector with a 5-pair AlGaN–GaN intermediate layer", *Phys. Stattus Solidi A,* Vol. 209, No. 3, pp. 579-584, 2012

[13] C. K. Wang, S. J. Chang, Y. K. Su, Y. Z. Chiou, S. C. Chen, C. S. Chang, T. K. Lin, H. L. Liu, and J. J. Tang, "GaN MSM UV Photodetectors With Titanium Tungsten Transparent Electrodes", *IEEE Trans. Electron Devices*, Vol. 53, No. 1, pp. 38-42, 2006.

[14] F. Xie, H. Lu, D. J. Chen, X. Q. Xiu, H. Zhao, R. Zhang, and Y. D. Zheng, "Metal–Semiconductor–Metal Ultraviolet Avalanche Photodiodes Fabricated on Bulk GaN Substrate", *IEEE Electron Device Lett.*, Vol. 32, No. 9, pp. 1260-1262, 2011.

[15] M. Girolami, P. Allegrini, G. Conte, D. M. Trucchi, V. G. Ralchenko, and S. Salvatori, "Diamond Detectors for UV

and X-Ray Source Imaging", *IEEE Electron Device Lett.*, Vol. 33, No. 2, pp. 224-226, 2012.

[16] P. E. Malinowski, J.-Y. Duboz, P. D. Moor, J. John, K. Minoglou, P. Srivastava, F. Semond, E. Frayssinet, B. Giordanengo, A. BenMoussa, U. Kroth, A. Gottwald, C. Laubis, R. Mertens, and C. V. Hoof, "AlGaN-on-Si-Based 10-μm Pixel-to-Pixel Pitch Hybrid Imagers for the EUV Range", *IEEE Electron Device Lett.*, Vol. 32, No. 11, pp. 1561-1563, 2011.